Online ISSN: 2981-0396 Print ISSN: 2981-0388

International Journal of Iron & Steel Society of Iran

Journal Homepage: https://journal.issiran.com/

Research Article

Modeling and Multi-Objective Optimization of Operating Parameters in Semi Autogenous Grinding Mill

M. Mohammadi Soleymani *[1], S. Mirzadeh [2]

[1] *Department of Mechanical Engineering, Payame Noor University, Tehran, Iran*
[2] *Department of Mathematics, University of Hormozgan, Bandar Abbas, Iran*

ARTICLE INFO

Keywords:

SAG mill, Multi-objective optimization, Artificial Neural Network, Genetic Algorithm.

Article history:

Received 29 May 2024
Received in revised form 01 July 2024
Accepted 01 September 2024

ABSTRACT

Mill optimization has many economic benefits. Semi autogenous grinding mills are complex multi-input and multi-output systems that are difficult to optimize. The purpose of this study is to examine the functions of the wear of lifters, power draw and product size distribution. The design variables are mill speed, ball filling, slurry concentration and slurry filling. To achieve this aim, a pilot mill was carried out. The experimental results used to create training cases for the artificial neural network and then the optimization of the design variables is conducted by multi-objective genetic algorithm. Level diagrams are then used to select the best solution from the Pareto front. Finally, the response surface methodology has been used to study the interaction between the design parameters. The results showed that the best grinding occurs at 70-80% of the critical speed and ball filling of 15-20%. Optimized grinding was observed when the slurry volume was 1-1.5 times of the ball bed voidage volume and the slurry concentration was 60-70%. Additionally, variables with the largest effect on the process are mill speed and ball filling.

1. Introduction

Due to the high consumption of energy and the high cost of grinding in the processing factories, Scientists always tried to use new methods to lower energy consumption of minerals per ton. Today, the use of autogenus (AG) and semi autogenous grinding (SAG) mill has become a priority for less energy per ton of ore. This mechanical machine is feeded with ore as a grinding agent that helps reduce the amount of ball consumption and prevent contamination in the circuit. This equipment requires less investment, and operating and maintenance cost is reduced. Moreover, the two final stages of crushing and primitive milling of these types of mills can be easily replaced, which ultimately lead to the reduction in the processing units, lateral operations and finally yields to more productivity in the processing units [1, 2].

In predicting and controlling the situation in the tumbling mills, many factors, such as multi-input, multi-output, nonlinearity of the system, are involved in large scale, which is why the processes of identifying and predicting the situation in mills create many difficulties [3, 4]. One of the best practices in identifying and modeling methods is to employ Soft Computing (SC) or Computational Intelligence (CI), which is used in many nonlinear systems with complex dynamic behaviors. Past studies are more about the modeling and simulation for semi-autogenous grinding mill circuits

*Corresponding author
Email: mmsoleymani@pnu.ac.ir
Address: Department of Mechanical Engineering, Payame Noor University, Tehran, Iran
1. Assistant Professor, 2. Assistant Professor

DOI: http://10.22034/IJISSI.2024.2030541.1294
Published by ISSI (Iron & Steel Society of Iran)

not the mill itself [5-8]. There are different types of advanced control systems such as multi target control [9, 10], model based and model predictive control [11, 12] and neural network [13-15]. To back up the advantages of this system, Bouch et al. described the application of the Optimizing Control System (OCS) at the Anglo-Gold Ashanti Gold plants [16].

Empirical and numerical studies have been conducted in the field of tumbling mills to examine the output variables of each mills such as the wear of liners [17, 18], power draw [19, 20], product size distribution [21, 22] and kinematics of mill contents [23], and it seems no study has been done to optimize and evaluate the effects of the parameters involved in this system so far. In mills, generally, experience, effort and error are adopted to design functional and operational parameters which are usually costly and time-consuming. The use of new combined methods such as laboratory simulation, along with techniques for optimizing and modeling the artificial neural network (ANN), machine learning techniques or fuzzy logic, allows for the best possible design to be created without incurring extra costs [24-26].

In order to optimize complex nonlinear problems that for instance occurs in the mills, it seem that the random methods with probability and statistics search algorithms are more efficient than adopting classical methods which is based on gradient functions. Because classical methods are only applicable to continuous functions and in addition to being able to be locked in local minima in these methods. Genetic algorithm is one of the well-known randomization methods that was invented by Holand in 1975 [27]. The genetic algorithm, with the ability to simultaneously search for different areas of the design space, can search for the optimized points of the complex problems, such as non-convex and discrete issues. A series of genetic algorithms based on Pareto points is called the multi-objective optimization evolution algorithm that can simultaneously optimize several objective functions. So far, many algorithms have been introduced and compared. The Non-dominated Sorting Genetic Algorithm II (NSGA-II), invented by Deb [28, 29] in 2001, is one of the most efficient algorithms that ensures the convergence and proper distribution of optimum points and its efficiency in solving various problems has been proven.

In this research, using the results of experimental simulation, a model was obtained by the artificial neural network in MATLAB software, and then this model was introduced as input function to multi-objective genetic algorithm NSGA-II, to optimize the parameters of the device for direction to achieve the minimum wear of liners, the maximum power draw of mill, and the minimum size product of the output of mill, and to achieve the related Pareto front. Due to the capabilities of ANN in modeling and predicting complex linear and nonlinear systems, this method is presented in the present study for SAG mill models.

2. Experimental Model

2.1. Test Condition

To model the behavior of the mill by using a neural network, a series of experimental results is required in terms of design variables. It's not possible to do these experiments on the real mill. Based on the geometric dimensional parameters of the pilot mill (Fig. 1.) to investigate the effect of several factors such as the speed of the mill, ball filling ratio, slurry density (concentration), slurry filling on parameters such as power draw, liner wear and product size distribution have been made.

A pilot mill (1000 mm diameter and 500 mm length) was used for experimentation. The pilot mill with the dimensions of one-tenth of the real mill was designed and built in Sarcheshmeh copper complex with dimensional similarity method. There are 15 lifters with 50mm height and face angle of 30˚. In the current work, the combination of the balls (40% of the balls with 60mm diameter, 40% of the balls with 40mm diameter and 20% of the balls with 25mm diameter) was used as grinding media. The mill motor was capable of changing the rotation permanently up to 100% of the critical speed. An electrical power analyzing device was used for measuring the mill power in terms of kW.The conditions of implementing the experiments are shown in Table 1.

Fig. 1. experimental pilot mill and mill contents.

Table 1. Experiments conditions for training the neural network.

Mill		
	Diameter	1000 mm
	Length	500 mm
	Speed	27, 29, 31, 33 and 35 rpm
	Critical speed of mill	42 rpm
	Fraction of critical speed (Φc)	0.65, 0.7, 0.75, 0.8 and 0.85
Lifters		
	Number	15
	Height	50 mm
	Face angle	30 degree
	Shape	Trapezoid, leg thickness 50 mm
Grinding media		
	Material	Chrome alloy steel
	Ball diameter	40% of the balls with 60mm diameter, 40% of the balls with 40mm diameter, and 20% of the balls with 25mm diameter
	Density	7800 kg/m3
	Total ball weight	176, 264, 352, 440 and 528 kg
	Ball filling (Jb)	0.1, 0.15, 0.2 , 0.25 and 0.3 fraction of mill volume
Feed		
	Material	Copper ore
	Particle size	$d_{100} = 25.4$, $d_{80} = 12.7$, $d_{50} = 8$ and $d_{10} = 0.3mm$
	Ore density	2700 kg/m3
	Slurry density	1340, 1460, 1610, 1790, and 2010 kg/m3
	Slurry concentration (C)	0.4, 0.5, 0.6, 0.7, and 0.8 (weight fraction of solid in slurry)
	Slurry filling (U)	0.5, 1, 1.5, 2 and 2.5 (as volume fraction of ball bed voidage)

In Table 1. four designed variables are defined and the conditions to carry out the tests are given. The first variable: mill speed to the critical speed (Φ_c); the second variable: the volume ratio of the balls to the total volume of mill (J_b); the third variable: the weight ratio of solids in the slurry to the total slurry weight (C) and the fourth variable: The slurry volume ratio to the volume of the balls (U). As all definitions of four designed variables are described, all variables are dimensionless, so that the results of this pilot mill can be used accurately for the real mill.

2.2. Calculate Target Functions

The input of mill feed is copper ore with a diameter of less than 1 inch, that dimension of 80% and 50% are below $1/2$ and $5/16$ inches, respectively. For each test condition, the mill is allowed to work for a few minutes, and then it is taken from the sample. After filter pressing, the specimens are placed in the dryer. When the specimens get dried and their weight is measured, we weigh them with 325 mesh peel and then weigh them again to see the weight of the particles below 44 microns. Subsequently, samples are placed in a vibrating machine with 25400 to 44-micron test shaker and the seed distribution is calculated. The size of 80% of the product dimensions is less than those calculated with P_{80}.

In a pilot mill with 1m diameter, in cascading motion, the ball velocity rapidly approaches 4m/s and it impacts at high speed in the toe region [30]. The kinetic energy of the balls with 60mm diameter and 0.88kg mass is approximately 7J. The energy of balls to grind the copper ore feed with dimensions of less than 1 inch and the average hardness is enough [31]. On experiment has been carried out to investigate whether the mill has been well designed in terms of operational parameters such as size and volume of the balls, number, height and face angle of the lifters, speed, etc or not. Therefore, 20% of the mill volume was filled with the balls. Besides, the slurry concentration is 60% and the slurry having the same volume of the balls was poured into the mill (U=1). Then, the mill worked for 10min with 80% of the critical speed. In Fig. 2. the distribution size of the mill product and the feed have been illustrated. As Fig. 2. shows, the mill grinding mechanism is a combination of impact and abrasive breakage mechanisms and P_{80}=115μm.

Two special liners were used to examine the wear (Fig. 3). These liners have specific locations for sample placement that could duly maintain the samples when they work in the mill. The samples were selected from soft steel and the samples are screwed. In order to measure the abrasion, the mass of the specimens was recorded with a precision scale of one-tenth of a milligram before the test was performed and after removing

the liner and performing the test, the specimens are removed from the liner and the mass is measured again. The wear of liner of the sample can be measured by calculating mass changes to the initial mass. Also, during the operation of the mill, the power draw was measured by the device (power analyzer) with an accuracy of 5 watts.

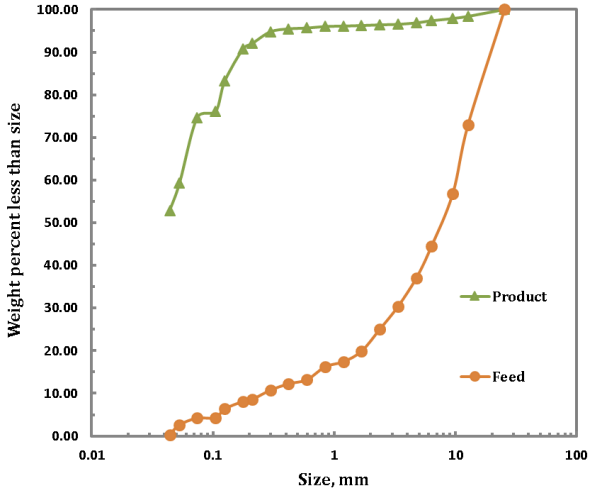

Fig. 2. Size distributions of feed and product ($J_b = 0.2, \Phi_C = 0.8, U = 1, C = 0.6$)

Fig. 3. Two specimens were made from ductile steel to measure wear.

3. Optimization

3.1. Problem definition

The general form of a multi-objective optimization problem is expressed as Eq. (1) [32].

$$\begin{aligned} &minimize\ F(\boldsymbol{X}) = \left(f_1(\boldsymbol{X}), f_2(\boldsymbol{X}), \dots, f_k(\boldsymbol{X})\right);\ \boldsymbol{X} \in \boldsymbol{S} \\ &h_i(\boldsymbol{X}) = 0 : i = 1\ to\ p \\ &g_j(\boldsymbol{X}) \le 0 : j = 1\ to\ q \\ &\boldsymbol{S} = \left\{\boldsymbol{X}\ 1\ h_i(\boldsymbol{X}) = 0; i = 1\ \ to\ \ p;\ g_j(\boldsymbol{X}) \le 0; j = 1\ \ to\ \ q\right\} \end{aligned} \quad \text{Eq. (1)}$$

Where k is the number of objective functions, p is the number of equal constraint, q is the number of inequalities, F(X) is the vector of the objective functions, $X=(x_1,x_2,\dots,x_n)$ is the vector of design variables and S is the feasible space. During the process of the mill, the speed of the mill, the amount of ball filling, the slurry concentration and the amount of slurry filling have a great influence on the wear of liners [17, 18], the power draw of the mill [19, 20], and the size of the particle production of the mill output [21, 22]. Therefore, considering these four quantities as design variables, one can simultaneously consider the optimal state of the mill. Table 2. shows the design variables and their range of variations. The ranges of input parameters have been selected from the previous studies [33]. In Table 3. the objective functions and optimal mode are observed as well.

3.2. Multi-objective optimization algorithm

In solving multi-objective optimization problems, the target functions are usually interconnected. This means that with the improvement of a function, another function drops, so that at the same time, you cannot see all the target functions to be on their best. To optimize simultaneously all of the objective functions, the concept of Pareto optimal points has been used [9]. The non-recessive points of Pareto are points that are not dominated by any other point. In other words, x_1 is a dominant point than x_2 if and only if Eq. (2) holds.

$$\begin{aligned} &f_i(x_1) \le f_i(x_2), \quad i = 1\ to\ k \\ &f_j(x_1) \le f_j(x_2), \quad j = 1\ to\ k \end{aligned} \quad \text{Eq. (2)}$$

In Eq. (2), k is the number of functions that must be minimized. Now, if there is no point in the design space that can overcome x_1 according to Eq. (2), then x_1 is a Pareto point. A set of Pareto points creates a Pareto front in the space of objective functions [10].

The general flowchart of the NSGA-II algorithm used in this research and its relation to the artificial neural network is presented in Fig. 4. In the NSGA-II algorithm, the initial population is randomly formed, and the values of the target functions, the number of selectable features, and the overall accuracy of the classification for each solution are computed. The objective functions are calculated by the neural network trained with the experimental results. Then, the members of the crowd are placed inside the fronts, so that members in the first front (F_1) are totally non-occupational set of target functions by other members of the current population. Members of the F_2 are also defeated by F_1 members on the same basis, and this trend continues with other fronts to allocate a rating based on its number to all members on each front. Then, for each member on each front, the crowding distance is calculated.

That way, first, the results are sorted for each function. To the points where the maximum and minimum value of this function is the target, the infinite interval is assigned. The crowding distance for other members of the population on each front is calculated according to the following relationships.

Table 2. Design variables, range of variables and levels of design variables.

Number	Design variables	Range of variables	Levels of design variables
1	Mill speed (Φ_c)	[0.65 - 0.85]	0.65, 0.7, 0.75, 0.8, 0.85
2	Ball filling (J_b)	[0.1 - 0.3]	0.1, 0.15, 0.2 , 0.25, 0.3
3	Slurry concentration (C)	[0.4 - 0.8]	0.4, 0.5, 0.6, 0.7, 0.8
4	Slurry filling (U)	[0.5 - 2.5]	0.5, 1, 1.5, 2, 2.5

Table 3. The objective functions and their optimal mode.

Number	Objective functions	Optimal mode
1	Power draw	Max
2	Wear of liner	Min
3	P_{80}	Min

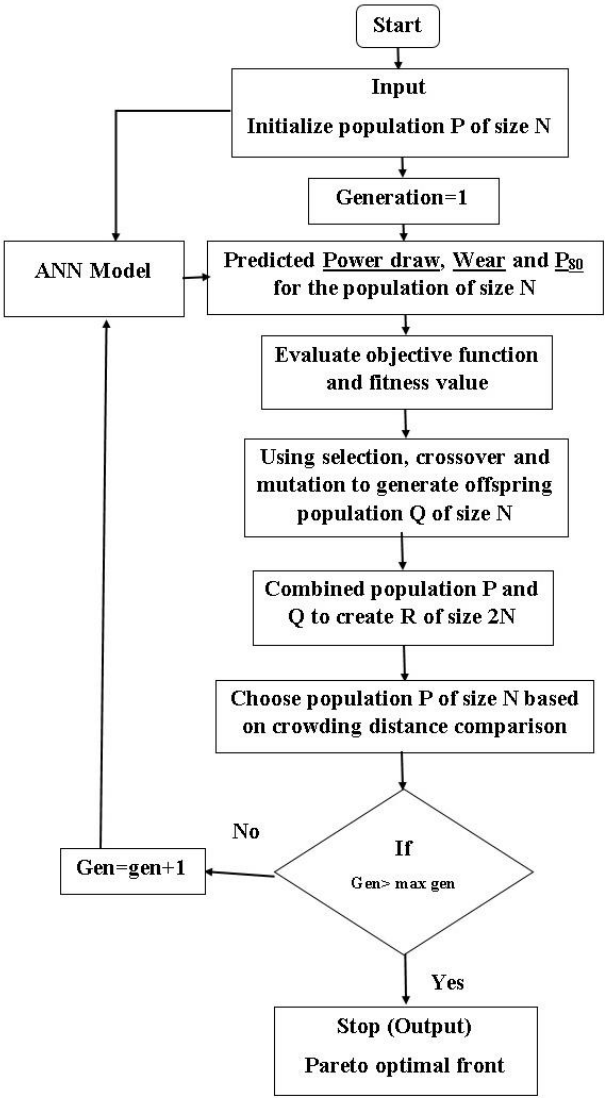

Fig. 4. Flowchart NSGA-II with ANN for optimization of SAG mill parameters.

$$cd_1^i = |\ f_1^{i+1} - f_1^{i-1}|\ /(f_1^{max} - f_1^{min}) \quad \text{Eq. (3)}$$

$$cd_2^i = |\ f_2^{i+1} - f_2^{i-1}|\ /(f_2^{max} - f_2^{min}) \quad \text{Eq. (4)}$$

$$cd(i) = cd_1^i + cd_2^i \quad \text{Eq. (5)}$$

In that cd(i), the crowding distance of the ith member on the fronts F, f_1^i and f_2^i, respectively, is the values of the first and second objective functions in the ith member on the frontal F and f_i^{min} and f_i^{max} respectively, is the lowest and highest value of the target function on F. In the following, using a binary competitive selection method, two solutions are randomly selected among the population, and a comparison is made between the two, and is the better is eventually selected. Selection criteria in the NSGA-II algorithm are primarily based on the response rank and, secondly, the overcrowding distance. Having the lesser extent in the rating of the response and the higher extent in the crowding distance are more desirable [34].

By repeating the binary selection operator on the population of each generation, a set of individuals of that generation is selected to participate in the crossover and mutation, and a population of children is created. In following this population is merged with the main population. New members of the population are first ranked in ascending order and then members of the same ranked population are sorted out based on the crowding distance in descending order, while the members of the population sorted primarily based on rank and secondarily ordering in terms of crowding distance. Equal to the number of people in the main population, members from the top of the arranged list are selected and the remaining members of the population are set aside. Selected members form the next generation of population, and the cycle in this section is repeated until the end of the term is fulfilled. Non-critical solutions obtained from multi-objective optimization problem are often known as the Pareto Front. None of the answers to the Pareto front is superior to each other, and each can be considered as an optimal decision [35, 36]. The parameters of Genetic Algorithm are shown in Table 4.

3.3. Artificial Neural Network

Due to the large number of possible states for testing or simulation, in order to train the artificial neural network, among all the different combinations in the design variables space, a number of suitable components were selected. Orthogonal arrays are statistical method designed to identify the system behavior by performing the least possible number of experiments that are used to determine the points of training of the neural network [37, 38]. For each design variable, five different levels are considered. By combining different levels according to the orthogonal arrays, 25 compounds that have good distribution in the design space were selected as training data for simulation. In addition to the training data, five other combinations that are called evaluation points are also randomly selected and simulated, which are used to check the validity of the network. Table 5. provides training points (1 to 25) and evaluation points (numbers 26 to 30).

To determine the optimal structure of the neural network, various networks were evaluated with the number of different layers and neurons. When the number of hidden neurons from a certain level increases, usually the accuracy of the training of the network increases, but its accuracy decreases in response to the evaluation points. So here's the network that has the least error in responding to the points of evaluation. The neural network used in this study is based on Fig. 5. of a feed forward net with a back propagation algorithm and a hidden layer which is consisted of 6 neurons. The number of neurons in the input layer is equal to the number of design variables, it means four neurons and the number of output layer neurons, are equal to the number of target functions, three neurons. The network is trained by the Levenberg-Marquardt method. The tangent sigmoid and linear functions are transient functions of the hidden and output layers, respectively.

An error-back propagation algorithm uses a gradient search method to minimize the mean square error (AMSE) of the network output. The method of calculating the mean squared error is based on Eq. (6) [39].

$$\text{AMSE} = \frac{1}{2N}\sum_{i=1}^{n}\sum_{j=1}^{m}\left(T_{ij} - O_{ij}\right)^2 \quad \text{Eq. (6)}$$

In this case, m is the number of neural network output neurons, N is the number of data used for network training, T is the target data for each neuron, and O is the predicted values for each output neuron.

Table 4. Parameters of the Genetic Algorithm.

Population	Mutation	Migration	Crossover	Generation
500	0.2	0.4	0.7	500

Table 5. Training points (numbers 1 to 25), evaluation points (numbers 26 to 30) and their test results.

Test number	Design variables				Target functions		
	Mill speed Φ_c	Ball filling J_b	Slurry concentration C	Slurry filling U	Wear (1/hr)	Power (kW)	P_{80} (μm)
1	0.65	0.1	0.4	0.5	0.001502	2.5	150
2	0.65	0.15	0.5	1	0.001676	3.34	180
3	0.65	0.2	0.6	1.5	0.00122	3.8	110
4	0.65	0.25	0.7	2	0.001976	4.2	160
5	0.65	0.3	0.8	2.5	0.002156	3.8	135
6	0.7	0.1	0.5	1.5	0.001756	2.84	132
7	0.7	0.15	0.6	2	0.001934	3.38	150
8	0.7	0.2	0.7	2.5	0.001453	4.5	115
9	0.7	0.25	0.8	0.5	0.001644	4.1	120
10	0.7	0.3	0.4	1	0.002012	5.33	110
11	0.75	0.1	0.6	2.5	0.002266	2.9	130
12	0.75	0.15	0.7	0.5	0.001696	4.1	120
13	0.75	0.2	0.8	1	0.001723	4	160
14	0.75	0.25	0.4	1.5	0.002283	5.1	150
15	0.75	0.3	0.5	2	0.001963	4.33	130
16	0.8	0.1	0.7	1	0.002263	3.52	170
17	0.8	0.15	0.8	1.5	0.001611	3.65	180
18	0.8	0.2	0.4	2	0.00202	4.67	150
19	0.8	0.25	0.5	2.5	0.002214	5.3	120
20	0.8	0.3	0.6	0.5	0.00165	5.5	155
21	0.85	0.1	0.8	2	0.001919	3	160
22	0.85	0.15	0.4	2.5	0.002472	4.14	132
23	0.85	0.2	0.5	0.5	0.001796	4.85	130
24	0.85	0.25	0.6	1	0.001789	5.4	170
25	0.85	0.3	0.7	1.5	0.002215	6.53	180
26	0.7	0.1	0.75	2.25	0.002319	6.6	190
27	0.75	0.15	0.7	1.5	0.002147	6.28	150
28	0.75	0.2	0.55	0.75	0.002052	4.85	150
29	0.8	0.25	0.60.	1.25	0.001896	5.33	175
30	0.8	0.3	0.45	1.5	0.002319	5.73	177

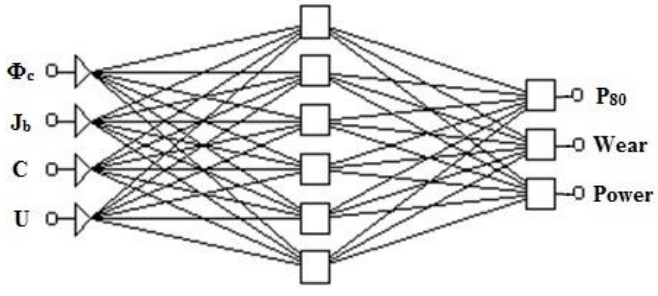

Fig. 5. A neural network designed to model experimental results.

An error propagation algorithm is a common method for training multi-layer neural networks. This algorithm has two different paths of sweep. The path that goes ahead, is called forward and the return path is also called the backward path. On the forward path, the input vector is sent to the input layer and an output vector is created based on the existing weights. The expected output value is compared with the actual value and the error value obtained from Eq. (6) is distributed using the Eq. (7)on the weights in the return path.

$$\Delta W_{ij} = -\frac{\partial E}{\partial W_{ij}}\alpha \qquad \text{Eq. (7)}$$

Which in the above relation is $0 < \alpha < 1$.

The coefficient α is a parameter that controls the convergence rate of the algorithm. The sweep routes are repeated so that the error value converges to the predetermined error value. In fact, the network is trained by distributing the error value obtained at each stage on the

previous weights and repeating the operation.

Regarding the distribution of the network output, the training data was normalized to all in the same range. In the first cycle of learning, weights of the network are randomly set, and the weights are repeatedly modified to repeat the cycles so that the network output with a negligible error is consistent with the results of the training data. The network error reached 0.0003 after 500 replies, indicating that the network has converged.

4. Results and discussion

4.1. Pareto optimal points

Linear regression between simulated points and network output was performed for each of the output parameters to evaluate the accuracy of the network training . Regression results show that the correlation coefficient for all graphs is higher than R=0.98, which indicates that the network has been well trained. Also, to evaluate the network's ability to model points outside the training area, five evaluation points were assessed by the neural network. Table 6. provides a comparison between the results of experimental data and output of the neural network for these five samples. The average network error for wearing liners, product seedlings, and power draw mill at the points of evaluation is 3.8%, 10.4% and 2%, respectively. Errors in the evaluation of liners wear and grain size may be due to its nonlinear relationship with the design data and the inadequacy of the training data, are higher than the evaluation error of the power draw. However, according to Table 6. the regression results for each of the output parameters in these five samples show that the correlation coefficient for all of them is higher than R=0.98. Therefore, it can be concluded that the neural network is duly able to evaluate the points within the design space with a high degree of speed and accuracy. Also the results of this research are completely consistent with the Neuro-Fuzzy method [40].

After training the artificial neural network by applying the results of pilot simulations and studying the accuracy and reliability of the network, this can be used as a cost function in the genetic algorithm. In each cycle, the generation is evaluated by the neural network and, if needed, is improved by the new generation and sent again to the neural network for evaluation. This cycle continues until the convergence criterion of the algorithm is met. The multi-objective optimization algorithm NSGA-II introduces Pareto's dominant points instead of an optimum point, and the designer can choose the desired design from the Pareto points according to his need and assessment. In order to combine the neural network and optimization algorithm, coding was used in MATLAB environment. After convergence of the algorithm, 18 optimal designs were obtained as Pareto points. Table 7. shows the pareto optimal points and their output values.

To calculate target functions in multi-objective genetic algorithm, neural network was used and the Pareto front which was obtained from it, is shown in Fig. 6. All Pareto points are somewhere optimal and none of them is superior to the other points, but one of these points should be selected for construction and implementation. Using graphical graphs is one of the easiest and most useful ways to help designers select the values of design variables. By plotting Pareto points and Pareto fronts, these graphs provide a better representation of the optimality of each of the points.

4.2. Choosing the best Layout

In this research, level diagrams have been used to select the best possible layout from Pareto points. To solve or tackle multi-objective optimization problems, Blasco et al introduced the level diagram in 2008. This is one of the ways in which the distance of the Pareto points to the ideal point (the best possible plan) is evaluated in accordance with Eq. (8) and the point where the lowest distance is introduced as the top plan [10]. This distance, the so-called Norm, is a criterion for choosing the best point. Different norms can be chosen for this purpose, with the use of ∞-norm here.

Table 6. Comparison between the results of test and output of the neural network for evaluation points.

Test number	P_{80} (μm)			Power draw (kW)			Wear (1/hr)		
	ANN	Test	Error (%)	ANN	Test	Error (%)	ANN	Test	Error (%)
26	165	190	13.2	5.94	6.06	2	0.002206	0.002319	4.9
27	167	150	11.3	6.1	6.28	2.8	0.002080	0.002147	3.1
28	170	150	13.3	5	4.85	3.1	0.002000	0.002052	2.5
29	165	175	5.7	5.26	5.33	1.3	0.001952	0.001896	2.9
30	162	177	8.5	5.67	5.73	1	0.002186	0.002319	5.7
Error	Correlation coefficient 0.98		Average error 10.4%	Correlation coefficient 0.99		Average error 2%	Correlation coefficient 0.99		Average error 3.8%

Table 7. Pareto optimal points and their output values.

Number	Pareto points				Pareto output		
	Mill speed Φ_c	Ball filling J_b	Slurry concentration C	Slurry filling U	Wear (1/hr)	Power (kW)	P_{80} (μm)
1	0.82	0.3	0.62	0.85	0.002019	5.23	190
2	0.84	0.29	0.68	1.15	0.001847	6.05	186
3	0.85	0.28	0.72	1.05	0.001952	5.84	175
4	0.85	0.29	0.71	0.95	0.001896	5.66	175
5	0.85	0.3	0.69	0.85	0.002019	5.79	177
6	0.82	0.27	0.65	1.2	0.002147	6.01	190
7	0.66	0.27	0.8	2.05	0.001452	4.49	150
8	0.67	0.26	0.75	2.5	0.001596	4.85	150
9	0.7	0.25	0.76	2.45	0.001319	5.33	175
10	0.66	0.27	0.8	2.25	0.001247	5.73	177
11	0.65	0.3	0.73	2.15	0.001652	6.06	190
12	0.65	0.29	0.71	2.35	0.001696	6.28	150
13	0.74	0.15	0.45	1.5	0.001919	5.65	120
14	0.75	0.21	0.55	1.75	0.002147	4.85	130
15	0.75	0.18	0.52	1.25	0.002052	5.33	117
16	0.77	0.22	0.48	1.65	0.001896	5.73	125
17	0.72	0.19	0.51	1.35	0.002019	6.06	132
18	0.78	0.18	0.4	1.15	0.002147	5.56	142

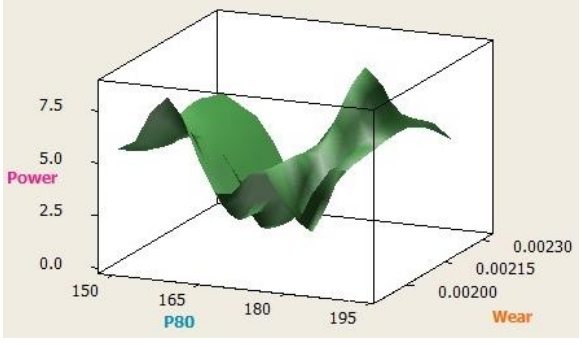

Fig. 6. The Pareto Front.

$$\infty - norm: f(x)_\infty = max\{\bar{f}_i(x)\}, \quad \text{Eq. (8)}$$

$$0 \le f(x)_\infty \le 1$$

$$\bar{f}_i(x) = \frac{f_i(x) - f_i^{min}}{f_i^{max} - f_i^{min}}, \qquad i = 1, \dots, m$$

$$\bar{f}_i(x) = \frac{f_i^{max} - f_i(x)}{f_i^{max} - f_i^{min}}, \qquad i = 1, \dots, n$$

$$0 \le \bar{f}_i(x) \le 1, \qquad i = 1, \dots, k$$

In Eq. (8), m is the number of objective functions to be minimized, n the number of target functions to be maximized, and k=m+n is the total number of target functions. After soft calculation of all Pareto points, each design variable and target function is drawn in norm places so that the horizontal axis is related to the design variable or target function and the vertical axis is relative to the norm values of the Pareto points.

Fig. 7. shows the surface diagrams of each of the design variables and target functions as compared to infinite norms. According to these graphs it can be seen that the point where the least norm value is closest to the ideal point and therefore is known as the highest point. According to Fig. 7. the lowest norm is about 0.54 and belongs to the point where the speed of mill, ball charge, slurry concentration and slurry filling value for this point are in the range of [0.75-0.80], [0.15-0.20], [0.6-0.7], and [1.00-1.50], which results in mill power draw (kW), liners wear (1 / hr), and P_{80} of final products (μm) are in the range of [5.5-6], [0.0016-0.002] and [120-150]. Also, sudden jumps of norm in the upper and lower bounds of design variables indicate that selection in these areas is not reasonable.

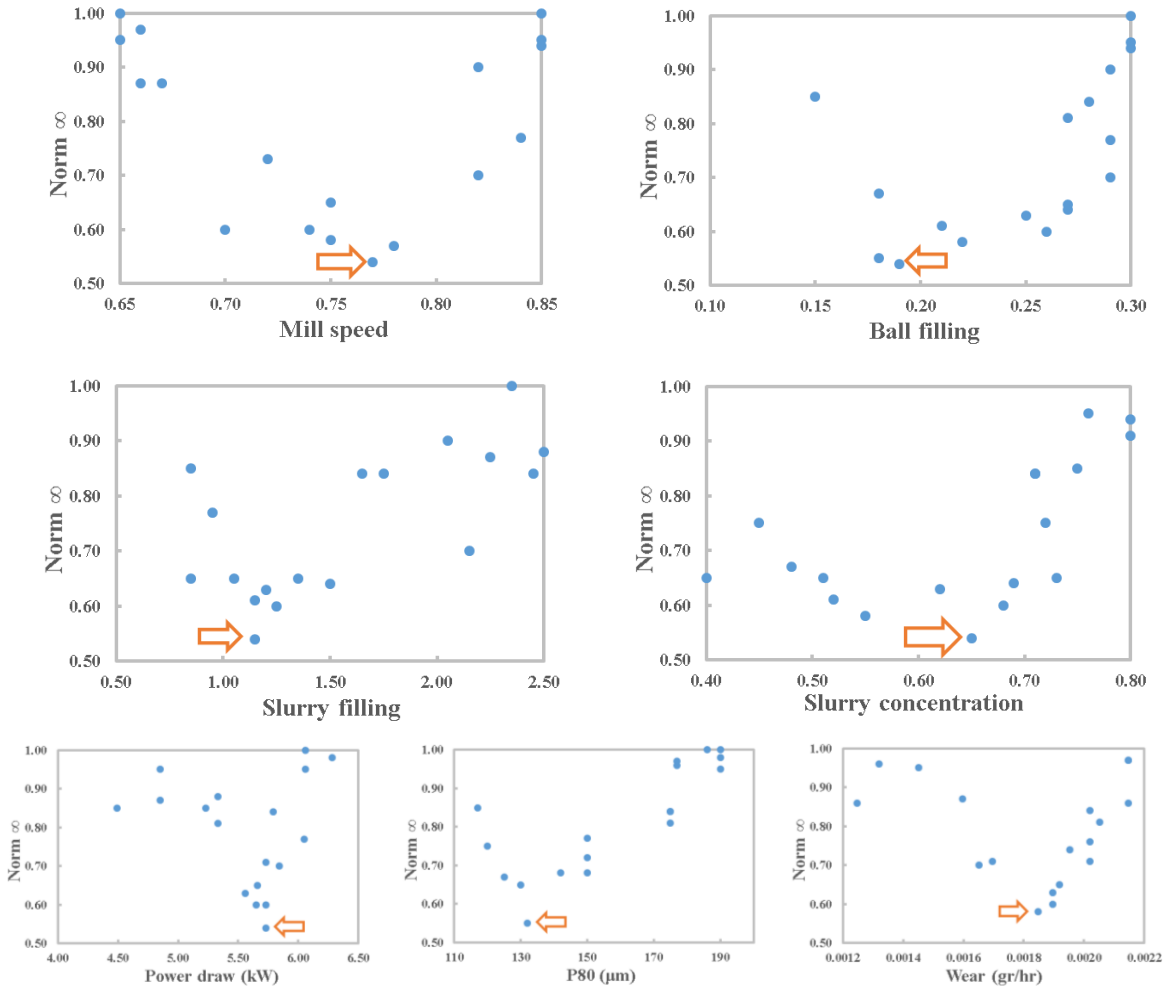

Fig. 7. Level diagrams related to design variables and target functions.

4.3. Sensitivity analysis

Understanding the effect of changing the design variables on the output of the process is very beneficial because it helps the designer to design better, change the design variables and create the desired design if needed. This research used the response level statistical method [37], and tried to create this vision for the problem designer. The answer surface method is a mathematical method for modeling and studying the effect of the parameters of a problem on its response. In this paper, using the response surface method, the importance of design parameters and the effect of the reaction between design parameters on the target functions are investigated. At first, for designing the test, using a composite design method with a combination of design variables, 25 experiments were considered. Then, using the trained neural network, the response to each of these experiments was obtained. Finally, with the fitting of a second order polynomial between all the experimental points, the equation of the level finds for each of the target functions. The second-order polynomials that are commonly used in the surface-response method are expressed in terms of Eq.(9).

$$Y = \beta_0 + \sum_{i=1}^{4} \beta_i X_i + \sum_{i=1}^{4} \beta_{ii} X_i^2 + \sum_{1 \le i < j \le 4} \beta_{ij} X_i X_j \qquad \text{Eq. (9)}$$

In the relation (9), β_0 ، β_i ، β_{ii} and β_{ij} are the polynomial fit coefficients obtained by the least squares method. X_i and X_j are design independent variables and Y is the response variable or the same objective function.

In Fig. 8. the equations and response levels associated with each of the target functions are shown in terms of design variables. In each of these levels, the two design variables remain constant in their mean values and the other two variables change within the permissible range. For example, to show the power draw mill in terms of speed and ball filling, the concentration and slurry filling remain constant at their average values of C=0.6 and U=1.5. Also, in order to plot the mill power in terms of the concentration and slurry filling, the speed and charge of the ball remain constant at their mean values of

Φ_c=0.75 and J_b=0.2.

By examining the surfaces of Fig. 8. it is seen that the speed of mill and the ball charge ratio significantly change the three target functions, but by changing the concentration and filling of the slurry, a smaller change in the response occurs. The power is directly related to the speed and ball filling. By increasing the slurry concentration up to 70% along with the increase in the slurry filling ratio up to U = 1, the power draw increases and then decreases. By increasing the volume and concentration of the slurry as well as increasing the charge of the ball, the wear rate of the liners decreases. Wear is directly related to the speed of the mill. The fine particles in the product of mill are reduced by increasing the volume and concentration of the slurry. By increasing the charge of the ball in the mill, the grain size becomes smaller. In the ball charging of 20% and 75% speed, the minimum P_{80} occurs.

To better investigate and determine the effect of the interaction of design variables on the final response, the Pareto diagram for each of the target functions is plotted using the Stat graphics software in Fig. 9. The length of each strip is proportional to the effect of that parameter on the final response. If the bar crosses the vertical line, it indicates that the corresponding parameter has a significant effect on the final response. The parameters that are directly related to the corresponding response are marked with a positive sign and the parameters that are inverse to the corresponding response are marked with a negative sign in front of them.

The study of Pareto diagrams shows that the speed of the mill and the ratio of ball charging have the greatest effect on the mill power draw, on the wear of liner, and also on the Product Size Distribution. It is also evident that the interaction between these two parameters is significant for all three objective functions. In the power and wear diagrams, the role of concentration and filling of slurry in the final response is low. Therefore, it can be said that the most influential parameters on the power draw, the wear of the liner and the grain size of the product are the ball filling and speed of the mill. Slurry concentrations and slurry filling have a minor role in the target functions.

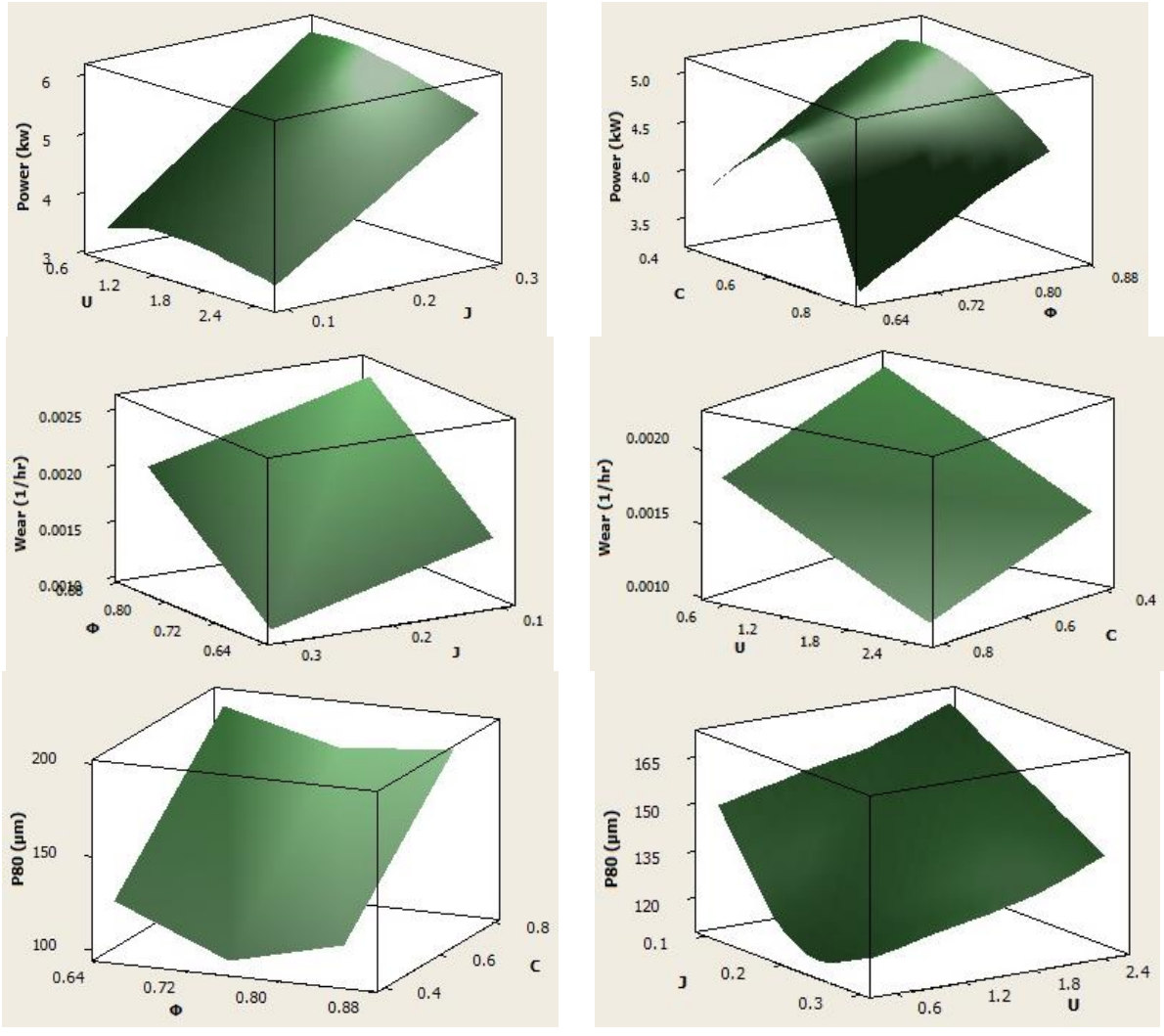

Fig. 8. Response levels for design variables.

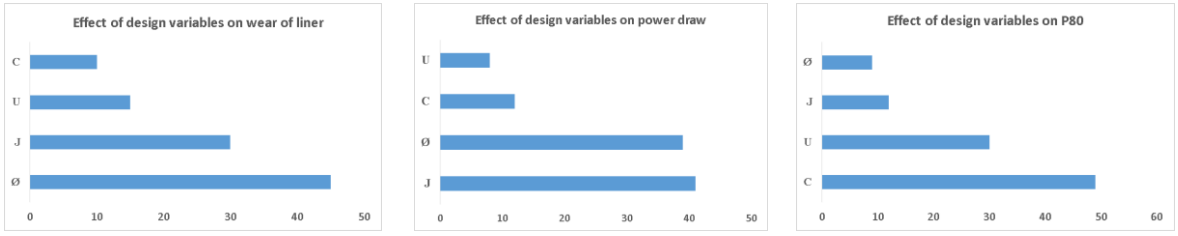

Fig. 9. The effect of design variables on target functions.

5. Conclusions

In this paper, multi-objective optimization of the operating parameters of SAG mills with a combination of experimental results, artificial neural network, and NSGA-II multi-objective genetic algorithm were studied. Also, analysis of response levels, the relationship between design variables, output functions, and the importance of each design parameter were investigated. The most important results of this research, which can be very useful for processing plants and mineral industries, are:

- The neural network is sufficiently efficient to act as a model for the performance of mill.
- The best selection ranges for mill speed, ball filling, slurry concentration and slurry filling ratio are in the range [0.75-0.8], [0.15-0.2], [0.6-0.7], and [1-1.5] respectively. The above values can be used in the industry.
- The power draw is directly related to the speed of the mill and the charge of ball. By increasing the slurry concentration up to 70% and increasing the slurry filling ratio up to 1.5, the power draw increases and then decreases.
- When the volume and concentration of the slurry and the charge of the ball are increased, the wear rate of the liner is reduced. Wear is directly related to the speed of mill.
- Small particles in the mill products are reduced when the volume and concentration of the slurry are increased. In the ball charging of 20% and 75% speed, the minimum P_{80} occurs.
- The most influential parameters on the power draw of the mill, the wear of liners, and the Product Size Distribution by the response surface method, are ball filling and speed of the mill.

Acknowledgments

This research was supported by NICICO. Special thanks to the generous helps of R&D and the concentrate unit of NICICO.

References

[1] Salazar J.L, Magne L, Acuna G, Cubillos F, Dynamic modelling and simulation of semi-autogenous mills. Minerals Engineering. 2009; 22(1): 70-7.
[2] Silva D.A, Tapia L.A, Experiences and lessons with advanced control systems for the SAG mill control in Minera Los Pelambres, IFAC Proceedings Volumes. 2009; 42(23): 25-30.
[3] Morrell S, A new autogenous and semi-autogenous mill model for scale-up, design and optimisation. Minerals Engineering. 2004; 17(3): 437-45.
[4] Ruel M, Fuzzy Logic Control on a SAG Mill, IFAC Proceedings Volumes. 2013; 46(16): 282-7.
[5] Hoseinian F.S, Faradonbeh R.S, Abdollahzadeh A, Rezai B, Soltani-Mohammadi S, Semi-autogenous mill power model development using gene expression programming, Powder Technology. 2017; 308: 61-9.
[6] Hadizadeh M, Farzanegan A, Noaparast M, A plant-scale validated MATLAB-based fuzzy expert system to control SAG mill circuits, Journal of Process Control. 2018; 70: 1-1.
[7] Hadizadeh M, Farzanegan A, Noaparast M, Supervisory fuzzy expert controller for sag mill grinding circuits: Sungun copper concentrator, Mineral Processing and Extractive Metallurgy Review. 2017; 38(3): 168-79.
[8] Chai T, Zhai L, Yue H, Multiple models and neural networks based decoupling control of ball mill coal-pulverizing systems, Journal of Process Control. 2011; 21(3): 351-66.
[9] Shi S, Xiong H, A hybrid immune genetic algorithm with tabu search for minimizing the tool switch times in CNC milling batch-processing. Applied Intelligence. 2022; 52(7): 7793-807.
[10] Blasco X, Herrero J.M, Sanchis J, Martínez M, A new graphical visualization of n-dimensional Pareto front for decision-making in multiobjective optimization, Information Sciences. 2008; 178(20): 3908-24.
[11] Chen X.S, Zhai J.Y, Li S.H, Li Q, Application of model predictive control in ball mill grinding circuit. Minerals Engineering. 2007; 20(11): 1099-108.
[12] Apelt T.A, Thornhill N.F, Inferential measurement of SAG mill parameters V: MPC simulation, Minerals Engineering. 2009; 22(12): 1045-52.
[13] Wu Y, Jin W, Ren J, Sun Z, A multi-perspective architecture for high-speed train fault diagnosis based on variational mode decomposition and enhanced multi-scale structure, Applied Intelligence. 2019; 49(11): 3923-37.

[14] Flament F, Thibault J, Hodouin D, Neural network based control of mineral grinding plants, Minerals engineering. 1993; 6(3): 235-49.
[15] Conradie A.V, Aldrich C, Neurocontrol of a ball mill grinding circuit using evolutionary reinforcement learning, Minerals engineering. 2001; 14(10): 1277-94.
[16] Bouché C, Brandt C, Broussaud A, Advanced control of gold ore grinding plants in South Africa, Minerals Engineering. 2005; 18(8): 866-76.
[17] Soleymani M, Fooladi M, Rezaeizadeh M, Bahiraie M, Experimental study of mill speed, charge filling, slurry concentration, and slurry filling on the wear of lifters in tumbling mills, Modares Mechanical Engineering. 2015; 15(4): 265-71.
[18] Omar Q.R, Valenzuela M.A, Estimation of Lifters Wear in Ball and SAG Mills using Neuro-Fuzzy Modeling, In 2018 IEEE Industry Applications Society Annual Meeting (IAS). 2018: 1-7.
[19] Soleymani M.M, Fooladi M, Rezaeizadeh M, Experimental investigation of the power draw of tumbling mills in wet grinding, Proceedings of the Institution of Mechanical Engineers, Part C: Journal of Mechanical Engineering Science. 2016; 230(15): 2709-19.
[20] Apelt T.A, Asprey S.P, Thornhill N.F, Inferential measurement of SAG mill parameters, Minerals engineering. 2001; 14(6): 575-91.
[21] Morrell S, A method for predicting the specific energy requirement of comminution circuits and assessing their energy utilisation efficiency, Minerals Engineering. 2008; 21(3): 224-33.
[22] Moys M.H, Grinding to nano-sizes: Effect of media size and slurry viscosity, Minerals Engineering. 2015; 74: 64-7.
[23] Soleymani M.M, Fooladi M, Rezaeizadeh M, Effect of slurry pool formation on the load orientation, power draw, and impact force in tumbling mills, Powder Technology. 2016; 287: 160-8.
[24] McCaffery K.M, Katom M, Craven J.W, Ongoing evolution of advanced SAG mill control at Ok Tedi. Mining, Metallurgy & Exploration. 2002; 19(2): 72.
[25] Fernandes M, Corchado J.M, Marreiros G, Machine learning techniques applied to mechanical fault diagnosis and fault prognosis in the context of real industrial manufacturing use-cases: a systematic literature review, Applied Intelligence. 2022: 1-35.
[26] Jiang Y, Chen J, Zhou H, Yang J, Xu G, Residual learning of the dynamics model for feeding system modelling based on dynamic nonlinear correlate factor analysis, Applied Intelligence. 2021; 51(7): 5067-80.
[27] Holland J.H, Adaptation in natural and artificial systems: an introductory analysis with applications to biology, control, and artificial intelligence. MIT Press. 1992.
[28] Deb K, Pratap A, Agarwal S, Meyarivan T.A, A fast and elitist multiobjective genetic algorithm: NSGA-II, IEEE transactions on evolutionary computation. 2002; 6(2): 182-97.
[29] Deb K, Multi-objective optimization, InSearch methodologies. 2014: 403-449.
[30] Rezaeizadeh M, Fooladi M, Powell M.S, Mansouri S.H, Weerasekara N.S, A new predictive model of lifter bar wear in mills, Minerals Engineering. 2010; 23(15): 1174-81.
[31] Tavares L.M, Breakage of single particles: quasi-static, Handbook of powder technology. 2007; 12: 3-68.
[32] Arora J.S, Introduction to optimum design, Elsevier; 2004.
[33] Jnr W.V, Morrell S, The development of a dynamic model for autogenous and semi-autogenous grinding, Minerals engineering. 1995; 8(11): 1285-97.
[34] Konak A, Coit D.W, Smith A.E, Multi-objective optimization using genetic algorithms: A tutorial. Reliability Engineering & System Safety. 2006; 91(9): 992-1007.
[35] Wang Z, Lu J, Chen C, Ma J, Liao X, Investigating the multi-objective optimization of quality and efficiency using deep reinforcement learning, Applied Intelligence. 2022:1-5.
[36] Li Y, Li W, Zhao Y, Li S, Hybrid multi-objective optimization algorithm based on angle competition and neighborhood protection mechanism, Applied Intelligence. 2022: 1-23.
[37] Vanderplaats, G.N, Numerical optimization techniques for engineering design: with applications. 1984; 1.
[38] Liu G, Zhou X, Xu X, Wang L, Zhang W, Fault diagnosis of diesel engine information fusion based on adaptive dynamic weighted hybrid distance-taguchi method (ADWHD-T), Applied Intelligence. 2022; 13:1-23.
[39] Mandal D, Pal S.K, Saha P, Modeling of electrical discharge machining process using back propagation neural network and multi-objective optimization using non-dominating sorting genetic algorithm-II, Journal of Materials Processing Technology. 2007; 186(1): 154-162.
[40] Mohammadi Soleymani M and Mirzadeh S, Multi-objective optimization of operating parameters in tumbling mill with Neuro-Fuzzy network, Modares Mechanical Engineering. 2020; 20(9): 2331-2341.